Published in final edited form as:

Int J Hyperthermia. 2018 May ; 34(3): 284–291. doi:10.1080/02656736.2017.1336675.

Hyperthermia-enhanced targeted drug delivery using magnetic resonance-guided focussed ultrasound: a pre-clinical study in a genetic model of pancreatic cancer

Navid Farr[a], **Yak-Nam Wang**[b], **Samantha D'Andrea**[c], **Frank Starr**[b], **Ari Partanen**[d], **Kayla M. Gravelle**[c], **Jeannine S. McCune**[e], **Linda J. Risler**[e], **Stella G. Whang**[c], **Amy Chang**[f], **Sunil R. Hingorani**[c,f], **Donghoon Lee**[g], and **Joo Ha Hwang**[c]

[a]Department of Bioengineering, University of Washington, Seattle, WA, USA;

[b]Applied Physics Laboratory, University of Washington, Seattle, WA, USA;

[c]Department of Medicine, University of Washington, Seattle, WA, USA;

[d]Philips, Clinical Science MR Therapy, Andover, MA, USA;

[e]Pharmacokinetics Laboratory, University of Washington, Seattle, WA, USA;

[f]Fred Hutchinson Cancer Research Center, Seattle, WA, USA;

[g]Department of Radiology, University of Washington, Seattle, WA, USA

Abstract

Purpose: The lack of effective treatment options for pancreatic cancer has led to a 5-year survival rate of just 8%. Here, we evaluate the ability to enhance targeted drug delivery using mild hyperthermia in combination with the systemic administration of a low-temperature sensitive liposomal formulation of doxorubicin (LTSL-Dox) using a relevant model for pancreas cancer.

Materials and methods: Experiments were performed in a genetically engineered mouse model of pancreatic cancer (KPC mice: LSL-Kras$^{G12D/+}$; LSL-Trp53$^{R172H/+}$; Pdx-1-Cre). LTSL-Dox or free doxorubicin (Dox) was administered via a tail vein catheter. A clinical magnetic resonance-guided high intensity focussed ultrasound (MR-HIFU) system was used to plan treatment, apply the HIFU-induce hyperthermia and monitor therapy. Post-therapy, total Dox concentration in tumour tissue was determined by HPLC and confirmed with fluorescence microscopy.

Results: Localized hyperthermia was successfully applied and monitored with a clinical MR-HIFU system. The mild hyperthermia heating algorithm administered by the MR-HIFU system resulted in homogenous heating within the region of interest. MR-HIFU, in combination with LTSL-Dox, resulted in a 23-fold increase in the localised drug concentration and nuclear uptake of

CONTACT Joo Ha Hwang Jooha@medicine.washington.edu Division of Gastroenterology, Department of Medicine, University of Washington, 1959 NE Pacific Street, Seattle, WA 98195, USA.

Disclosure statement

Ari Partanen is paid employee of Philips. All other authors report no declarations of interest.

doxorubicin within the tumour tissue of KPC mice compared to LTSL-Dox alone. Hyperthermia, in combination with free Dox, resulted in a 2-fold increase compared to Dox alone.

Conclusion: This study demonstrates that HIFU-induced hyperthermia in combination with LTSL-Dox can be a non-invasive and effective method in enhancing the localised delivery and penetration of doxorubicin into pancreatic tumours.

Keywords

Focused ultrasound; hyperthermia; pancreatic cancer; KPC mouse model; magnetic resonance imaging

Introduction

Pancreatic cancer is expected to become the second leading cause of cancer-related deaths in the USA by 2020 [1,2]. The most common (85%) and deadly form of pancreas cancer is pancreatic ductal adenocarcinoma (PDA). More than 53 000 patients in the USA will be diagnosed with pancreatic cancer in 2016, and almost 42 000 deaths are predicted to occur in the same year. The 5-year over-all survival rate is 8%, with the average life expectancy after diagnosis with metastatic disease being 3–6 months. Surgery offers the only potential for cure, yet less than 20% of patients that present with non-metastatic tumours are amenable to resection [3], and the median survival after resection is still only 13–20 months [4–6].

For patients with non-resectable tumours (~85%), the standard-of-care has been chemotherapy with or without radiation therapy. Although these therapies have been successful in arresting tumour growth in pre-clinical trials [7,8], clinically they merely extended survival and/or relieved symptoms to a modest degree. Indeed, they often only result in increases in survival on the order of weeks [9]. The discrepancy between pre-clinical and clinical results is thought to be due to the large differences in tumour histopathology present in the xenograft and syngeneic autograph animal models used in pre-clinical studies compared to the actual disease seen in humans [10].

The ineffectiveness of conventional chemotherapeutics in PDA is thought to be largely due to the extensive stromal desmoplasia [11] and, in particular, to inordinately elevated interstitial gel fluid pressures resulting from water in complex with high concentrations of hyaluronic acid [12,13]. These pressures, in turn, cause widespread vascular collapse and subsequent hypoperfusion. Interestingly, the vessels in PDA are otherwise structurally and functionally intact [14], unlike the “leaky” vessels described in allograft and xenograft systems. As such, the traditional transplantable tumour models do not accurately depict the fluid mechanics and complexity in human PDA (reviewed in [15,16]), resulting in their inability to predict clinical efficacy in drug trials. The recently developed genetically engineered mouse model, in which mutant Kras and p53 alleles are expressed in pancreatic cells, develops tumours that closely resembles the pathophysiology and molecular features found in human PDA [17,18]. This animal therefore provides a more realistic model with which to evaluate the potential for future therapies, especially in drug delivery.

In addition to the physical barriers to drug delivery, the high drug dose required to achieve clinically effective cytotoxicity in tumours often causes damage to actively propagating non-malignant cells, resulting in serious side effects [19]. The development of novel strategies for targeted drug delivery systems using clinically relevant animal models is therefore urgently needed to combat this deadly disease.

Mild hyperthermia in combination with chemotherapy or other therapeutic molecules has been used to treat cancers, with results indicating improved tumour responses and overall survival [20]. Not only does mild hyperthermia have a sensitising effect on tumour cells, but also the slight increase in temperature can increase the permeability of tumour vasculature, increasing blood and interstitial fluid flow and in turn resulting in the equilibration of interstitial fluid pressure [21]. Localized hyperthermia treatment used in combination with encapsulated drug can result in preferential accumulation of the encapsulated drug in the heated tumour [22–24], reducing the potential for systemic toxicity. Once within the tumour, the encapsulated chemotherapeutic agent can be triggered to release (e.g. temperature, enzyme or pH change). There are several temperature-sensitive liposomes (TSLs) specifically designed to release the encapsulated drug with the application of mild hyperthermia [25,26]. The use of these liposomes would therefore lead to the localised distribution of the drug within the heated tumour.

Of the current technologies used to administer localised hyperthermia, high intensity focussed ultrasound (HIFU) provides the most precise targeting of the heated region without excess heating of collateral tissue [27,28]. The ability to monitor the treatment with MR-guidance allows precise temporal and spatial control of the therapy [29]. Several studies have shown the success of targeted drug delivery in solid tumours when hyperthermia is applied using HIFU in conjunction with a TSL [19,30–33]. This therapy combination therefore offers a promising solution in treating PDA. The objective of this study was to evaluate the enhancement of drug delivery using MR-guided HIFU-induced hyperthermia, in conjunction with a systemically administered low-temperature sensitive liposome loaded with doxorubicin (LTSL-Dox) in a clinically relevant mouse model for PDA.

Materials and methods

Chemotherapeutic agents

A lyso-lecithin containing an LTSL-Dox formulation (ThermoDox®, Celsion Corp., Lawrenceville, NJ) with 2 mg doxorubicin/mL was obtained through a collaborative agreement. Doxorubicin hydrochloride (Doxorubicin HCl, BioVision Inc., Milpitas, CA) was used as the non-liposomal drug (Dox).

MR-HIFU system

A clinical MR-HIFU system (Sonalleve V1, Philips, Vantaa, Finland) on a clinical MRI system (Achieva 3 T, Philips) was used for image acquisition, treatment planning, hyperthermia administration and monitoring. Anatomical and temperature imaging at a spatial and temporal resolution sufficient for mild hyperthermia in mice was facilitated by using a custom small animal research coil setup [34].

Animal model and study design

All experimental procedures were approved by the Institutional Animal Care and Use Committee of the University of Washington, Seattle, WA. A genetically engineered strain of *Mus musculus* with mutations of *KrasG12D, Trp53R172H* and *Pdx-1-Cre* recombinase targeted to the pancreas (KPC mouse model) was used [13,17].

Tumour bearing KPC mice were enrolled into the study when the tumour reached 1 cm in diameter. Mice were assigned randomly into MR-HIFU hyperthermia treated and no hyperthermia treatment (control) groups (n = 4 in each group). Doxorubicin was delivered in the form of the temperature sensitive liposomal doxorubicin (LTSL-Dox) or nonliposomal doxorubicin (Dox). A doxorubicin dose of 15 mg/kg was used to facilitate the detection (visualisation of Dox uptake in addition to providing a higher signal for the HPLC quantification) after treatment.

Experimental procedures

The study animal was anaesthetised and the abdomen and back was shaved, depilated and washed before being placed in a custom made animal holder (Figure 1). Degassed ultra-sound gel was placed around and on top of the animal and an acoustic absorber was placed on the back of the animal to control the exit of the ultrasound beam. The animal was instrumented to monitor core body temperature and respiration (SAII Instruments, Stony Brook, NY).

Once the animal was placed within the MRI coil, a survey scan was performed followed by a susceptibility sensitive scan (T1-weighted 3D steady-state gradient-echo; TR/TE: 15/12 ms; FA: 10°; FOV: 150 × 150 × 40 mm^3; voxel size: 1.1 × 1.1 × 2.0 mm^3; slices: 20; acquisition time: 2 min) to check for the presence of air bubbles in the ultrasound beam path. HIFU treatment was planned on a proton density-weighted image set acquired with a fast field echo [orientation: coronal; TR/TE: 1791/13 ms; FA: 20°; FOV: 40 × 48 mm^2; voxel size: 0.25 × 0.25 × 1.00 mm^3; parallel imaging (SENSE) factor: 2 (in RL direction), saturation bands: 2; slices: 20; acquisition time: 5 min].

An ellipsoidal (4 × 4 × 10 mm^3) treatment volume (referred to as the “treatment cell”) was placed inside the mouse tumour. A low-power test sonication (continuous wave ultra-sound, frequency = 1.2 MHz, acoustic power 10 = W; duration = 20 s; corresponding to 180 W/cm^2) was performed prior to hyperthermia sonication to identify any miss-registration of the planned treatment location. Once the treatment was planned and co-registered, animals were slowly injected with 15 mg/kg LTSL-Dox or Dox via a tail vein catheter. Therapeutic sonication (continuous wave ultrasound, acoustic power = 7 W) was started within 5 min post-injection.

Temperature of the treatment site was monitored via continuous 2D fast field echo-echo planar imaging pulse sequence [TR 50 ms, TE = 20 ms, flip angle 20°, voxel = 0.9× 0.9 × 4.0 mm^3, FOV = 100 × 100 mm^2, EPI-factor = 7, parallel imaging (SENSE) factor = 2 (RL), saturation bands = 3, dynamic scan time = 1.8s one tomographic slice perpendicular and parallel to the beam axis, both centred on the target volume. Temperature maps were calculated online using the MR phase images and the proton resonance frequency shift

(PRFS) thermometry method, and displayed on the therapy control workstation [35]. The temperature images were corrected for baseline drift by subtracting the drift calculated from an unheated region in the ultrasound gel from the actual temperature data. A binary feedback control algorithm was used to switch the transducer power on and off to keep the temperature within a specific goal range (T_{min} = 41 °C, T_{max} = 42.5 °C) [36,37]. The target temperature was based upon the release characteristics provided by Celsion Corporation. The mean temperature during treatment was calculated automatically within the treatment region of interest (ROI). All hyperthermia treatments were analysed post-treatment in Matlab (MathWorks, Natick, MA). The mean temperature, highest 10th percentile (T10), lowest 10th percentile (T90) and standard deviation (SD) in target region were analysed from the coronal slice to assess temperature accuracy and uniformity [37]. Following each 5- or 10-min interval of mild hyperthermia, the sonication was stopped to allow recalibration of the temperature elevation measurements to readjust the baseline temperature in the software, as well as to evaluate the condition of the animal. The body core temperature of the animal range between 35 and 38 °C during hyperthermia. Sonication was continued for 2 or 5 more minutes as needed (total hyperthermia time: 15 min). A total hyperthermia time of 15 min was chosen as longer periods of hyperthermia can lead to a decrease in blood flow [38]. Following treatment, the mouse was removed from the system, at least 10 min of treatment, the vasculature was flushed with saline, the mouse euthanized and the tumour was collected for evaluation.

Liquid chromatography with tandem mass spectrometry

Tissue was taken through the entire thickness of the tumour to ensure that any inhomogeneities within the tumour were equally sampled. Quantification of doxorubicin was achieved by HPLC as described previously [39,40]. Briefly, samples were homogenised in a mixture of 0.1% formic acid and acetonitrile. An internal standard (20 ng epirubicin) was added. The samples were run on a liquid-chromatography-mass spectrometry system (6410B triple quadrupole mass spectrometer coupled to a 1290 series UPLC system; Agilent Technologies, Santa Clara, CA). An eight-point calibration curve was created by spiking blank tumour with doxorubicin and then processing it in the same manner as the samples. The relationship between the peak heights of the doxorubicin and epirubicin and their respective concentrations was analysed by second-order polynomial regression. The correlation coefficient was used to evaluate the linearity of the calibration curves and was >0.995 in all experiments.

Fluorescent microscopy and histological evaluation

After removing a small sample for the quantification of doxorubicin, the rest of the tumour was embedded in optimum cutting temperature medium. Serial, 5-μm-thick sections were cut (CM1950, Leica Biosystems Inc., Buffalo Grove, IL) to evaluate doxorubicin distribution using fluorescence microscopy, for qualitative assessment of stromal tissue using Masson’s trichrome staining and blood vessel visualisation by immunohistochemical staining for CD31 (CD31, 1/100 dilution, BD Biosciences, San Jose, CA; Alexa Fluor 594 goat anti-rat secondary, 1/500, ThermoFisher Scientific, Waltham, MA). All sections were examined using a Nikon H550 L light microscope (Nikon, Melville, NY). Doxorubicin uptake was visualised using a custom filter set (480/40 nm Ex; 605/50 nm Em; dichroic, 505

lp), and blood vessels were visualised with a Texas Red filter set. All images were acquired with the same exposure times.

Statistics

Following data reduction, tissue drug concentration values are reported as the median drug concentration per weight of tissue. Within each injection dosage group, the doxorubicin concentrations were compared between groups of animals using the Mann–Whitney *U* test.

Results

MR-guided hyperthermia

The mild hyperthermia heating algorithm administered by the MR-HIFU resulted in a narrow target temperature range with a mean temperature of 41.2 ± 1.3 °C(T10 = 41.3–43.1 °C, T90 = 39.0–39.7 °C), which was homogeneous within the ROI(Figure 2(A,B)). The target temperature was achieved within 9.6 ± 7.8 s (mean ± SD, Figure 2(C)). The mean temperature for animals treated with DOX (41.09 ± 1.4 °C) was not significantly different than animals treated with TSL-DOX (41.27 ± 1.75 °C). In a post-treatment analysis comparing an unheated region of gel and mouse, no significant difference was found in the mean temperatures due to movement.

Drug concentration

The median doxorubicin concentrations achieved within the tumour are presented in Table 1. Hyperthermia resulted in a 23-fold increase in the median doxorubicin concentration in the tumours (Figure 3) when delivered in the form of LTSL-Dox compared to animals with no hyperthermia applied ($U = 0$, $p < 0.05$, $r = 0.82$). When the doxorubicin was delivered in the non-liposomal form (Dox), hyperthermia resulted in a 2-fold increase over drug alone ($U = 1$, $p < 0.05$, $r = 0.71$). Both of these increases were statistically significant. Despite the limited size of the study, the effect size was large for both comparisons. The delivery of doxorubicin in the LTSL form resulted in a 2-fold increase in tumour doxorubicin concentration when combined with hyperthermia treatment compared with non-LTSL doxorubicin ($U = 8$, $p = 0.5$, $r = 0$). However, this increase was not significantly different. Comparing the administration of LTSL-Dox with hyperthermia to Dox alone, there was a 4-fold increase in Dox concentration delivered to the tumour ($U = 4$, $p = 0.12$, $r = 0.41$). Although this increase was not significant, the effect size was small for this comparison. Without hyperthermia, there was an almost 5-fold greater concentration of doxorubicin when it was administered as non-liposomal doxorubicin which was statistically significant ($U = 2$, $p < 0.05$, $r = 0.61$).

Fluorescence microscopy

The quantitative HPLC data were supported by qualitative evaluations. Representative fluorescence images of KPC pancreata from the groups that were administered 15 mg Dox/kg in the form of LTSL-Dox with and without the application of MR-HIFU were compared with sequential sections stained with Masson’s trichrome to correlate drug uptake with the structure of the tumours (Figure 4). The characteristically robust desmoplastic response was observed in KPC pancreata even in tumour-adjacent regions with pre-invasive

disease only. None of the tumours showed damage caused by the application of HIFU-mediated hyperthermia. Specifically, the sections were evaluated for structural disruption and coagulative necrosis. In the mice administered LTSL-Dox or Dox without hyperthermia, there was no evidence of doxorubicin nuclear uptake in any region of the tumour. Dox uptake was observed within the tumour cells as well as the cells within the desmoplastic stroma with the application of hyperthermia with either LTSL-Dox or Dox. In some tumours, there appeared to be preferential drug uptake in the periphery of the tumour compared with the centre of the tumour; however, this was more pronounced with the administration of Dox + MR-HIFU (Figure 4).

Discussion

The efficacy of using hyperthermia induced by HIFU to enhance the delivery of doxorubicin in combination with a low-temperature liposome was evaluated in a clinically relevant model of PDA. The KPC mouse model closely recapitulates the characteristic of PDA which are responsible for ineffectiveness of traditional chemotherapeutics.

The use of a clinical MR-HIFU system enabled accurate tissue delineation in the planning phase, monitoring and control of mild hyperthermia within a narrow temperature range (41.2 ± 1.3 °C), and subsequent delivery to a target area <1 cm in diameter. Maintaining the temperature below 43 °C may be critical, as vascular shut-down can occur at higher temperatures, eliminating some of the benefit of the hyper-thermia treatment [41]. For the LTSL-Dox to have maximal effect, the liposomal drug must first reach the target tissue via the vascular system and then release its payload within the heated tissue, resulting in high local concentrations of the drug that can then penetrate into the tissue due to high concentration gradients.

The results from this study demonstrated that systemic administration of a LTSL loaded with doxorubicin followed by targeted hyperthermia induced by focussed ultrasound and monitored using MR-thermometry significantly increased the median doxorubicin accumulation within the targeted tumour tissue by 2-fold compared to systemic administration of the same dose of doxorubicin in a non-encapsulated form. The observed increase in drug accumulation was supported by fluorescence microscopy, which demonstrated nuclear uptake of doxorubicin in the heated tumours and widespread accumulation.

Two mechanisms can be responsible for increasing drug accumulation: hyperthermia-induced vascular changes and localised drug release. Mild hyperthermia (40–43 °C) has been shown to increase tumour blood flow [42–44] and increase tumour vascular permeability [45]. It is likely that the increase in drug concentration when combining hyperthermia with the LTSL drug results from both the hyperthermia-induced changes in tumour vascular characteristics (permeability and blood flow) and the localised high concentration of the bio-available drug being released within the vasculature [46]. When mild hyperthermia was used in combination with Dox, there was an increase in the median doxorubicin accumulation within the tumour tissue, but the increase (up to 2-fold) was not as large as that observed with the LTSL-Dox (up to 23-fold). The use of hyperthermia to

increase blood flow and vessel permeability would enable a greater amount of the small molecule doxorubicin to enter the tumour tissue and extravasate from the vessels to reach the tumour cells.

In this study, continuous wave HIFU was successful in delivering mild hyperthermia to a small localised area to enhance drug delivery. However, other HIFU induced bioeffects such as cavitation can also be taken advantage of to further enhance drug penetration. In a previous study, pulsed HIFU has been used to mechanically disrupt stroma resulting in an increase in permeability of stroma in pancreas tumours and a subsequent increase in drug penetration (up to 4.5-fold increase) [40]. It is therefore possible that drug penetration could be even further enhanced by a combination of HIFU induced mild hyperthermia and mechanical disruption.

In this study, the animal was sacrificed almost immediately after hyperthermia. It is likely that there will be differences in drug uptake depending on the time of sacrifice after injection, with the longer times potentially yielding a larger amount of Dox uptake [47]. This is 80–100% release of drug in 20–40 s at 41.3 °C [48] and the one pass circulation time of a mouse is approximately 15 s [49]. Therefore, it is likely that the amount of Dox in the heated tumour would be greater if the mice were allowed to survive for some hours after treatment. Although these studies did not capture the total possible Dox delivered, the short time point after treatment was sufficient for Dox release and nuclear uptake for the Thermodox case, while enabling a measureable differentiation between the non-heated and heated mice given free Dox. The prolonged effects of the hyperthermia treatment will be further evaluated in survival animals.

One limitation of this study is the small number of animals in each group. However, despite the small sample size, the effect size calculated for the increases that were found to be significant, suggesting that the effect was real (effect size >0.5). Another limitation is the amount of tissue that was heated and the potential for motion artefact. Given that this study was performed on a clinical system designed for human treatment, it is possible that more than just the tumour tissue was heated and that movement due to breathing would affect the temperature monitoring. However, this additional tissue heating was minimised by monitoring an image slice placed within the post-focal region to ensure that this tissue did not reach temperatures that would result in activation of the LTSL-Dox. In addition, this heating would not be an issue when treating patients as the application of hyperthermia to normal tissue should be acceptable and the treatment to ensure a good margin of treatment is indeed desired. By positioning the lungs in different plane than the tumour using acoustically transparent gel pads under the thoracic region of the mouse, artefacts due to respiratory motion was minimised as indicated by post-treatment analysis. We anticipate that this will not be an issue in the clinic where there are established protocols for the management of respiratory motion. Another limitation is that a high doxorubicin dose (15 mg/kg) was used in this study to enable visualisation of the doxorubicin uptake. In future studies, a lower dose will be administered to evaluate survival benefit and the effects on tumour growth. Finally, although gemcitabine is the current standard-of-care for pancreatic cancer, there is currently no clinically approved thermosensitive liposomal form of the drug. The clinical use of doxorubicin may have been impeded by poor biodistribution and

subsequent dose-limiting toxicity [50]. As such doxorubicin is not currently used for the treatment of pancreatic cancer. However, there are numerous studies evaluating novel delivery methods of doxorubicin to improve local accumulation without systemic toxicity which could lead to the use of doxorubicin for pancreas cancer in the future [51–53].

This study shows that HIFU-induced mild hyperthermia in combination with a low-temperature-sensitive liposomal doxorubicin can be effective in substantially enhancing the penetration of doxorubicin into pancreatic tumours in the KPC mouse model. Building on these promising results, subsequent studies will focus on the effectiveness of the treatment on survival rates and tumour growth in addition to combining the different therapeutic effects of HIFU (heat and cavitation).

Conclusion

In this study, we demonstrated that hyperthermia induced by HIFU could be successfully applied, controlled and monitored using a clinical MR-HIFU system to increase the targeted release of a drug encapsulated in a low-temperature thermo-sensitive liposome in tumours of a realistic mouse model of pancreatic ductal adenocarcinoma. This, in turn, resulted in a significant increase in the bioavailable drug concentration (up to 23-fold between LSTSL-Dox with heat compared to LTSL-Dox alone) and a subsequent increase in intratumoural penetration. In addition, the application of mild hyperthermia alone appears to increase delivery of free doxorubicin (2-fold increase) but not to the same extent as the encapsulated drug.

Acknowledgements

Thermodox was provided by Celsion Corporation (Lawrenceville, NJ) and the mouse coil was provided by Philips (The Netherlands). We would like to thank Prof. Holger Grüll, Dr. Nicole M. Hijnen and Ms. Esther C. M. Kneepkens for their assistance.

Funding

This work was supported by the Focused Ultrasound Foundation and US National Institutes of Health [NIH R01CA154451 and R01 CA161112] from the National Cancer Institute (NCI).

References

[1]. Rahib L, Smith BD, Aizenberg R, et al. (2014). Projecting cancer incidence and deaths to 2030: the unexpected burden of thyroid, liver, and pancreas cancers in the United States. Cancer Res 74:2913–21. [PubMed: 24840647]

[2]. American Cancer Society. (2016). Cancer facts and figures 2016. Atlanta, GA: American Cancer Society.

[3]. Malik NK, May KS, Chandrasekhar R, et al. (2012). Treatment of locally advanced unresectable pancreatic cancer: a 10-year experience. J Gastrointest Oncol 3:326–34. [PubMed: 23205309]

[4]. Geer RJ, Brennan MF. (1993). Prognostic indicators for survival after resection of pancreatic adenocarcinoma. Am J Surg 165:68–72. [PubMed: 8380315]

[5]. Lim JE, Chien MW, Earle CC. (2003). Prognostic factors following curative resection for pancreatic adenocarcinoma: a population-based, linked database analysis of 396 patients. Ann Surg 237:74–85. [PubMed: 12496533]

[6]. Ueda M, Endo I, Nakashima M, et al. (2009). Prognostic factors after resection of pancreatic cancer. World J Surg 33:104–10. [PubMed: 19011933]

[7]. Yu M, Tannock IF. (2012). Targeting tumor architecture to favor drug penetration: a new weapon to combat chemoresistance in pancreatic cancer? Cancer Cell 21:327–9. [PubMed: 22439929]

[8]. Yu X, Zhang Y, Chen C, et al. (2010). Targeted drug delivery in pancreatic cancer. Biochim Biophys Acta 1805:97–104. [PubMed: 19853645]

[9]. Burris HA, Moore MJ, Andersen J, et al. (1997). Improvements in survival and clinical benefit with gemcitabine as first-line therapy for patients with advanced pancreas cancer: a randomized trial. J Clin Oncol 15:2403–13. [PubMed: 9196156]

[10]. Izeradjene K, Hingorani SR. (2007). Targets, trials, and travails in pancreas cancer. J Natl Compr Cancer Netw 5:1042–53.

[11]. Erkan M, Hausmann S, Michalski CW, et al. (2012). The role of stroma in pancreatic cancer: diagnostic and therapeutic implications. Nat Rev Gastroenterol Hepatol 9:454–67. [PubMed: 22710569]

[12]. DuFort CC, DelGiorno KE, Carlson MA, et al. (2016). Interstitial pressure in pancreatic ductal adenocarcinoma is dominated by a gel-fluid phase. Biophys J 110:2106–19. [PubMed: 27166818]

[13]. Provenzano PP, Cuevas C, Chang AE, et al. (2012). Enzymatic targeting of the stroma ablates physical barriers to treatment of pancreatic ductal adenocarcinoma. Cancer Cell 21:418–29. [PubMed: 22439937]

[14]. Jacobetz MA, Chan DS, Neesse A, et al. (2013). Hyaluronan impairs vascular function and drug delivery in a mouse model of pancreatic cancer. Gut 62:112–20. [PubMed: 22466618]

[15]. Provenzano PP, Hingorani SR. (2013). Hyaluronan, fluid pressure, and stromal resistance in pancreas cancer. Br J Cancer 108:1–8. [PubMed: 23299539]

[16]. DuFort CC, DelGiorno KE, Hingorani SR. (2016). Mounting pressure in the microenvironment: fluids, solids, and cells in pancreatic ductal adenocarcinoma. Gastroenterology 150:1545–57.e2. [PubMed: 27072672]

[17]. Hingorani SR, Wang L, Multani AS, et al. (2005). Trp53R172H and KrasG12D cooperate to promote chromosomal instability and widely metastatic pancreatic ductal adenocarcinoma in mice. Cancer Cell 7:469–83. [PubMed: 15894267]

[18]. Olive KP, Tuveson DA. (2006). The use of targeted mouse models for preclinical testing of novel cancer therapeutics. Clin Cancer Res 12:5277–87. [PubMed: 17000660]

[19]. Dromi S, Frenkel V, Luk A, et al. (2007). Pulsed-high intensity focused ultrasound and low temperature-sensitive liposomes for enhanced targeted drug delivery and antitumor effect. Clin Cancer Res 13:2722–7. [PubMed: 17473205]

[20]. Issels RD, Lindner LH, Verweij J, et al. (2010). Neo-adjuvant chemotherapy alone or with regional hyperthermia for localised high-risk soft-tissue sarcoma: a randomised phase 3 multicentre study. Lancet Oncol 11:561–70. [PubMed: 20434400]

[21]. Park K (2013). Improved tumor targeting by mild hyperthermia. J Control Release 167:220. [PubMed: 23534993]

[22]. Kong G, Anyarambhatla G, Petros WP, et al. (2000). Efficacy of liposomes and hyperthermia in a human tumor xenograft model: importance of triggered drug release. Cancer Res 60:6950–7. [PubMed: 11156395]

[23]. Kong G, Dewhirst MW. (1999). Hyperthermia and liposomes. Int J Hyperthermia 15:345–70. [PubMed: 10519688]

[24]. Needham D, Anyarambhatla G, Kong G, Dewhirst MW. (2000). A new temperature-sensitive liposome for use with mild hyper-thermia: characterization and testing in a human tumor xenograft model. Cancer Res 60:1197–201. [PubMed: 10728674]

[25]. Landon CD, Park JY, Needham D, Dewhirst MW. (2011). Nanoscale drug delivery and hyperthermia: the materials design and preclinical and clinical testing of low temperature-sensitive liposomes used in combination with mild hyperthermia in the treatment of local cancer. Open Nanomed J 3:38–64. [PubMed: 23807899]

[26]. Ta T, Porter TM. (2013). Thermosensitive liposomes for localized delivery and triggered release of chemotherapy. J Control Release 169:112–25. [PubMed: 23583706]

[27]. Maloney E, Hwang JH. (2015). Emerging HIFU applications in cancer therapy. Int J Hyperthermia 31:302–9. [PubMed: 25367011]

[28]. Haar GT, Coussios C. (2007). High intensity focused ultrasound: physical principles and devices. Int J Hyperthermia 23:89–104. [PubMed: 17578335]

[29]. Negussie AH, Yarmolenko PS, Partanen A, et al. (2011). Formulation and characterisation of magnetic resonance imageable thermally sensitive liposomes for use with magnetic resonance-guided high intensity focused ultrasound. Int J Hyperthermia 27:140–55. [PubMed: 21314334]

[30]. de Smet M, Heijman E, Langereis S, et al. (2011). Magnetic resonance imaging of high intensity focused ultrasound mediated drug delivery from temperature-sensitive liposomes: an in vivo proof-of-concept study. J Control Release 150:102–10. [PubMed: 21059375]

[31]. Salomir R, Vimeux FC, de Zwart JA, et al. (2000). Hyperthermia by MR-guided focused ultrasound: accurate temperature control based on fast MRI and a physical model of local energy deposition and heat conduction. Magn Reson Med 43:342–7. [PubMed: 10725875]

[32]. Staruch RM, Hynynen K, Chopra R. (2015). Hyperthermia-mediated doxorubicin release from thermosensitive liposomes using MRHIFU: therapeutic effect in rabbit Vx2 tumours. Int J Hyperthermia 31:118–33. [PubMed: 25582131]

[33]. Treat LH, McDannold N, Vykhodtseva N, et al. (2007). Targeted delivery of doxorubicin to the rat brain at therapeutic levels using MRI-guided focused ultrasound. Int J Cancer 121:901–7. [PubMed: 17437269]

[34]. Hijnen N, Langereis S, Grull H. (2014). Magnetic resonance guided high-intensity focused ultrasound for image-guided temperature-induced drug delivery. Adv Drug Deliv Rev 72:65–81. [PubMed: 24463345]

[35]. Ishihara Y, Calderon A, Watanabe H, et al. (1995). A precise and fast temperature mapping using water proton chemical shift. Magn Reson Med 34:814–23. [PubMed: 8598808]

[36]. Enholm JK, Kohler MO, Quesson B, et al. (2010). Improved volu-metric MR-HIFU ablation by robust binary feedback control. IEEE Trans Bio-Med Eng 57:103–13.

[37]. Partanen A, Yarmolenko PS, Viitala A, et al. (2012). Mild hyperthermia with magnetic resonance-guided high-intensity focused ultra-sound for applications in drug delivery. Int J Hyperthermia 28:320–36. [PubMed: 22621734]

[38]. Olsen DR, Singstad TE, Rofstad EK. (1999). Effects of hyperthermia on bioenergetic status and phosphorus T1S in human melanoma xenografts monitored by 31P-MRS. Magn Reson Imaging 17:1049–56. [PubMed: 10463656]

[39]. Al-Abd AM, Kim NH, Song SC, et al. (2009). A simple HPLC method for doxorubicin in plasma and tissues of nude mice. Arch Pharm Res 32:605–11. [PubMed: 19407979]

[40]. Li T, Wang YN, Khokhlova TD, et al. (2015). Pulsed high-intensity focused ultrasound enhances delivery of doxorubicin in a preclinical model of pancreatic cancer. Cancer Res 75:3738–46. [PubMed: 26216548]

[41]. Hildebrandt B, Wust P, Ahlers O, et al. (2002). The cellular and molecular basis of hyperthermia. Crit Rev Oncol Hematol 43:33–56. [PubMed: 12098606]

[42]. Horsman MR, Overgaard J. (1997). Can mild hyperthermia improve tumour oxygenation? Int J Hyperthermia 13:1417.

[43]. Song CW, Park H, Griffin RJ. (2001). Improvement of tumor oxygenation by mild hyperthermia. Radiat Res 155:515–28. [PubMed: 11260653]

[44]. Song CW, Park HJ, Lee CK, Griffin R. (2005). Implications of increased tumor blood flow and oxygenation caused by mild temperature hyperthermia in tumor treatment. Int J Hyperthermia 21:761–7. [PubMed: 16338859]

[45]. Kirui DK, Mai J, Palange AL, et al. (2014). Transient mild hyperthermia induces E-selectin mediated localization of mesoporous silicon vectors in solid tumors. PLoS One 9:e86489. [PubMed: 24558362]

[46]. Grull H, Langereis S. (2012). Hyperthermia-triggered drug delivery from temperature-sensitive liposomes using MRI-guided high intensity focused ultrasound. J Control Release 161: 317–27. [PubMed: 22565055]

[47]. de Smet M, Hijnen NM, Langereis S, et al. (2013). Magnetic resonance guided high-intensity focused ultrasound mediated hyper-thermia improves the intratumoral distribution of temperature-sensitive liposomal doxorubicin. Invest Radiol 48:395–405. [PubMed: 23399809]

[48]. Mills JK, Needham D. (2005). Lysolipid incorporation in dipalmitoylphosphatidylcholine bilayer membranes enhances the ion permeability and drug release rates at the membrane phase transition. Biochim Biophys Acta 1716:77–96. [PubMed: 16216216]

[49]. Debbage PL, Griebel J, Ried M, et al. (1998). Lectin intravital per-fusion studies in tumor-bearing mice: micrometer-resolution, wide-area mapping of microvascular labeling, distinguishing efficiently and inefficiently perfused microregions in the tumor. J Histochem Cytochem 46:627–39. [PubMed: 9562571]

[50]. Minchinton AI, Tannock IF. (2006). Drug penetration in solid tumours. Nat Rev Cancer 6:583–92. [PubMed: 16862189]

[51]. Yagublu V, Caliskan N, Lewis AL, et al. (2013). Treatment of experimental pancreatic cancer by doxorubicin-, mitoxantrone-, and irinotecan-drug eluting beads. Pancreatology 13:79–87. [PubMed: 23395574]

[52]. Mita MM, Natale RB, Wolin EM, et al. (2015). Pharmacokinetic study of aldoxorubicin in patients with solid tumors. Invest New drugs 33:341–8. [PubMed: 25388939]

[53]. Manzoor AA, Lindner LH, Landon CD, et al. (2012). Overcoming limitations in nanoparticle drug delivery: triggered, intravascular release to improve drug penetration into tumors. Cancer Res 72:5566–75. [PubMed: 22952218]

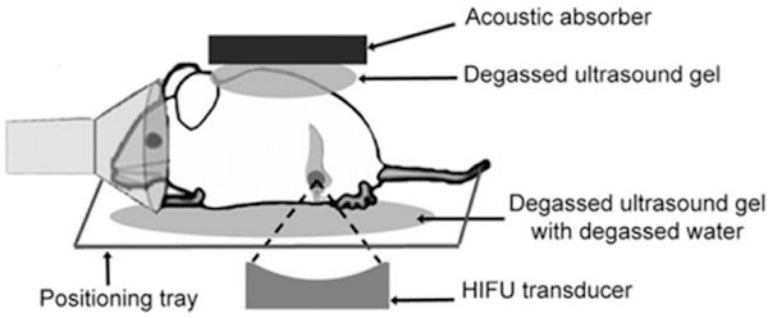

Figure 1.

In vivo experimental setup. Mice were placed on the positioning tray within the MR receive coil. Acoustic coupling was achieved by using distilled degassed water and degassed ultrasound gel. An acoustic absorber, coupled with ultrasound gel, was placed on the animal's back to control the exit beam and minimise movement. Respiration was monitored by an MR-compatible small animal monitoring system.

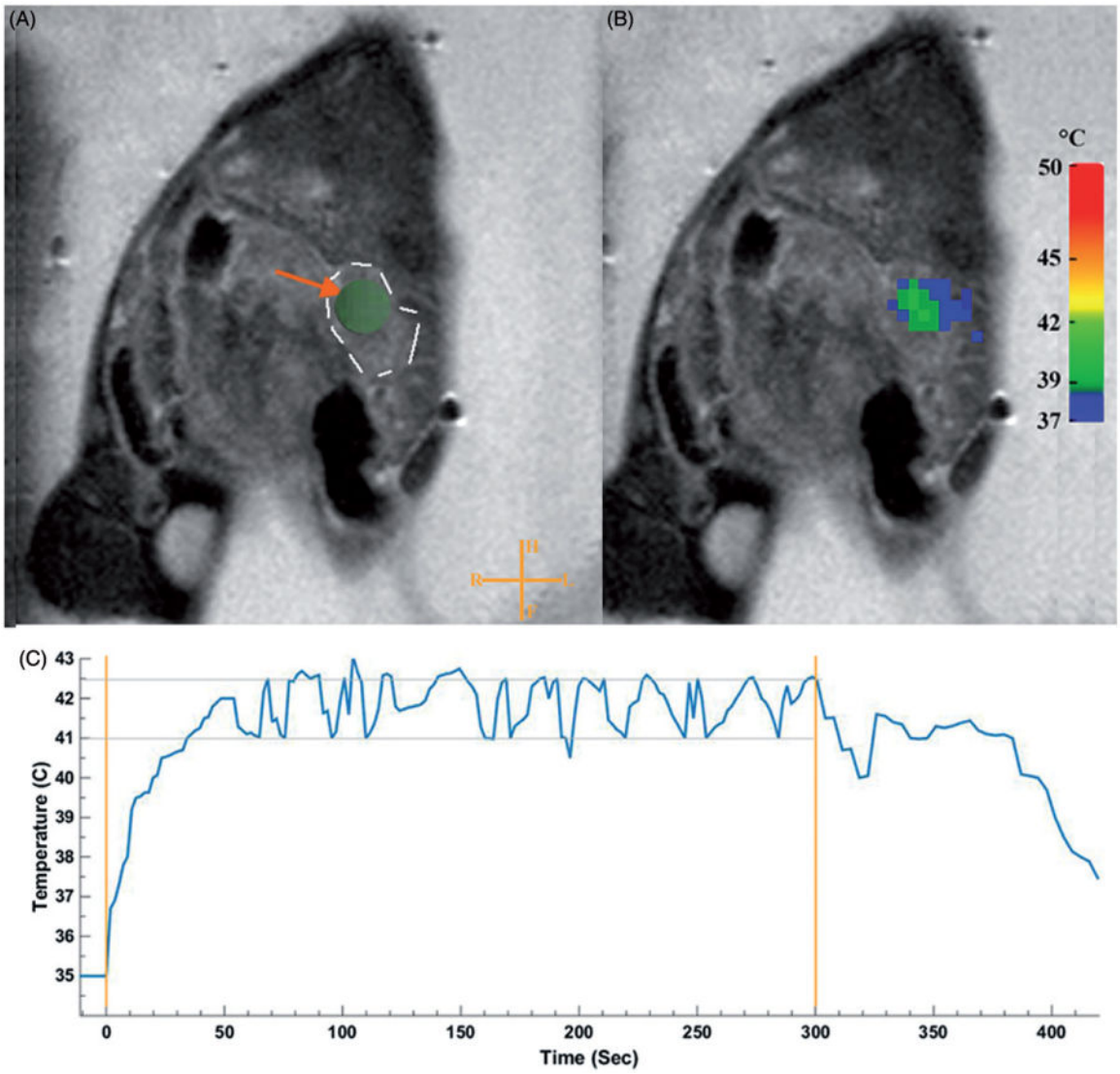

Figure 2.

Planning and temperature mapping for image-guided hyperthermia. The KPC tumour was identified on the planning images in the tail of the pancreas (A). The ROI was placed in the centre of the tumour. A dashed line to outline the tumour has been added to show the reader the tumour border. Real-time MRI-based temperature monitoring using the PRFS method shown in colour overlaid on the planning image (B). Representative mean temperature in the target region during a sonication (C). Stable mild hyperthermia was achieved in the target region through binary feedback control of temperature. An algorithm was utilised to keep the temperature in the range of 41–42.5 °C (horizontal lines) within the ROI (4 mm diameter). Orange vertical lines represent the start and end of the sonication.

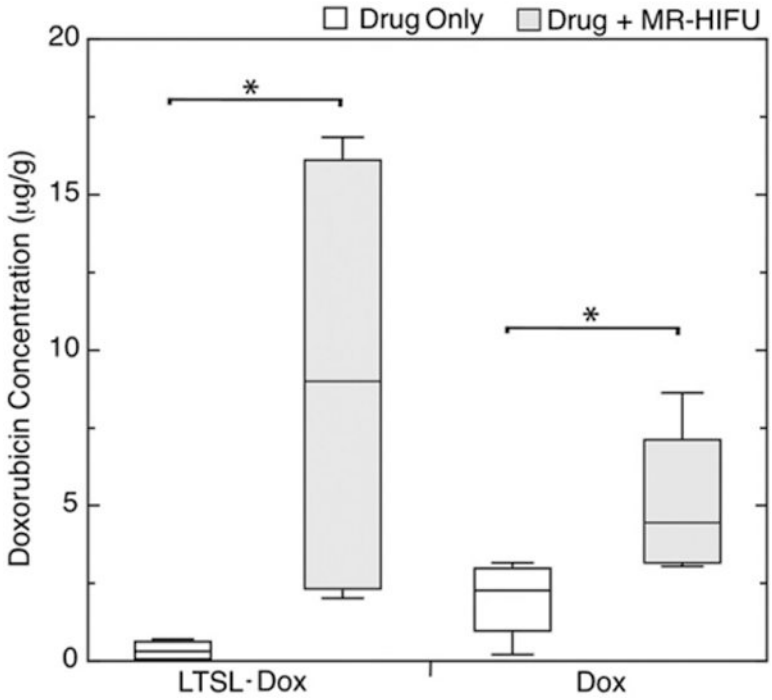

Figure 3.

Box-and-Whisker plot of doxorubicin (Dox) concentration in the tumours of KPC mice treated with 15 mg Dox/kg low-temperature-sensitive liposomal doxorubicin (LTSL-Dox) and non-liposomal doxorubicin (Dox), with and without the application of MR-HIFU. *Denotes significance at the $p < 0.05$ level.

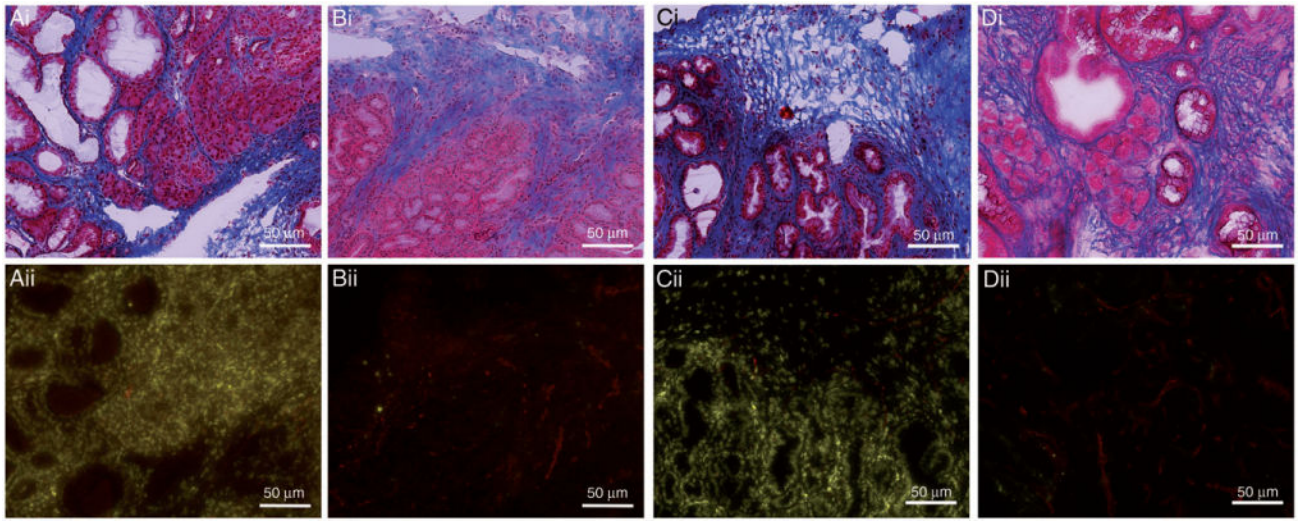

Figure 4.

Representative images of serial sections stained with Masson's trichrome (i) and fluorescent imaging (ii). Images demonstrate the distribution of doxorubicin and blood vessels within pancreatic tumours treated with LTSL-Dox + MR-HIFU (A); LTSL alone (B); DOX + MR-HIFU (C) OR Dox alone (D).

Table 1.

Median doxorubicin concentration [interquartile range] measured in pancreatic tumours following different treatment regimens (n = 4 in each group).

Treatment	Median doxorubicin concentration [interquartile range] (μg/g)
LTSL-Dox	0.31 [0.07–0.58]
LTSL-Dox + MR-HIFU	9.00 [2.48–15.73]
Dox	2.27 [1.35–2.89]
Dox + MR-HIFU	4.44 [3.22–6.37]